

# 1 Introduction

Climate change has become a major issue for nowadays generations. The continuously increasing emissions of greenhouse gases cause growing problems. Amongst others, these are sea-level rise, global temperature rise, warming oceans, shrinking ice sheets, declining arctic sea ice, glacial retreat and ocean acidification due to the absorption of carbon dioxide [1]. Climate change is driven by the emission of various greenhouse gases such as carbon dioxide ( $\text{CO}_2$ ), methane ( $\text{CH}_4$ ), nitrous oxide ( $\text{N}_2\text{O}$ ) and much more [2]. With an annual emission of 36.2 Gt in 2017 [3] and a fraction of 72 % of all greenhouse gases [4],  $\text{CO}_2$  is the most important driving force. Around 90 % of the  $\text{CO}_2$  released by human activities comes from combustion of fossil-fuels and production of cement [3].

To reduce the emissions of greenhouse gases different new technologies have been developed and implemented for energy generation. Some of them are carbon capture and storage (CCS) technologies. In combustion processes using CCS technologies fuels are still burned but the produced  $\text{CO}_2$  is captured separately and not released into the atmosphere. Subsequently, the  $\text{CO}_2$  can be stored in  $\text{CO}_2$  deposits or used for other processes. CCS technologies are bridging technologies that offer the further usage of fossil-fuels without or with reduced greenhouse gas emissions. By this they contribute to the mitigation of climate change.

One of the CCS technologies is the chemical looping combustion (CLC) process. In CLC the  $\text{CO}_2$  produced during combustion of carbon containing matter is separated from the combustion air. Thus, it possesses the advantage of the off-gas treatment for extraction of  $\text{CO}_2$  being obsolete to reach low carbon emissions. To realize the CLC process two reactors must be coupled. An oxygen carrier (OC) is circulating between these reactors. One of the reactors is passed through by air. The oxygen carrier, which is usually a metal/metal-oxide, is oxidized by the oxygen in this air reactor. Thus, the off-gas of this reactor contains air components only with a reduced fraction of oxygen and can be released to the atmosphere. The oxygen carrier is then transported into the second reactor. Here, the oxygen carrier is reduced and the released oxygen reacts with the fuel. The main components produced during combustion in this fuel reactor are  $\text{CO}_2$  and steam. The off-gas of the fuel reactor is treated by oxygen polishing to oxidize other combustion products like carbon monoxide, hydrogen or hydro

---

carbons. Then the water can be condensed in a further process step and CO<sub>2</sub> can be compressed and purified [5]. Finally, the depleted oxygen carrier is recirculated into the air reactor and the process repeats continuously.

Realization of the CLC process usually takes place in a system of interconnected fluidized bed reactors. Plants in different setups have been erected as summarized by Adánez *et al.* [5]. The fluidized bed reactors can be operated in the bubbling, the turbulent and the fast fluidized bed regimes.

Turbulent fluidized beds feature some advantages in comparison to other fluidized bed regimes, such as high solids hold-ups, high heat and mass transfer rates and limited axial gas mixing [6]. With its characteristic properties, the turbulent fluidized bed regime finds – besides CLC – a wide range of application in other processes. The most prominent example is the regenerator of the Fluid Catalytic Cracking (FCC) process [6, 7].

For the construction of large CLC plants it is necessary to find a fluidized bed design that provides high efficiency not only on a laboratory scale but also at industrial scale. To guarantee this, detailed understanding about the fluid dynamic behavior in the fluidized bed and the chemical reaction behavior is necessary. Models are often used for the prediction of the chemical conversion rates. For sufficient predictions, these models must be capable of overcoming the challenges that come with the process scale-up. Fluidized bed reactor models often consist of a fluid dynamic sub-model and one that predicts the complex chemical reaction behavior. Several models describing the fluid dynamic properties of turbulent fluidized beds are available in literature using different approaches [6]. Nevertheless, most of these models have been developed for processes where fine particles are used. These particles mostly belong to group A according to Geldart's classification. In contrast to this, the metal oxides usually used in CLC have larger particle sizes and densities. They show different fluidization behavior than group A particles and are classified as group B. Thus, most of the models for turbulent fluidization in literature give insufficient predictions of fluid dynamic properties like the local solids hold-up. There is a lack of models and information about the fluid dynamic behavior for particles belonging to group B according to Geldart's classification in the turbulent fluidization regime.

For this reason, it is the scope of this work to obtain detailed information about the fluid dynamic behavior of turbulent fluidized beds with particles of Geldart's group B in a thorough experimental study. Furthermore, a fluid dynamic sub-model is developed from the data measured to be able to model a turbulent fluidized bed included into the CLC process.

To predict fluidization behavior sufficiently in laboratory, as well as in large scale facilities, experiments are carried out in fluidized beds of different sizes

ranging from 0.05 m up to 1 m in diameter. Superficial gas velocities in the facilities are adjusted to reach states from bubbling, over turbulent, up to fast fluidization. Thereby, regimes are identified and their transitions are quantified. Different bed materials belonging to group B are used with main focus on a fraction of quartz sand having a Sauter mean diameter of 188  $\mu\text{m}$ .

Pressure fluctuations recorded in the different fluidized beds are evaluated. Furthermore, capacitance probes are used and with them solids concentrations, bubble properties and phase hold-ups are determined.

The information gathered from the measurements are used to correlate trends of several characteristic fluidization parameters. Finally, the resulting correlations are used to introduce a model describing the fluidization behavior of turbulent fluidized beds using particles of Geldart's group B.



## 2 State of the Art

In this chapter an overview about the current state of the art in gas-solid turbulent fluidized beds is given. The different flow regimes and the fluidization behavior of different particles are briefly summarized to provide a classification of turbulent fluidized beds using particles of Geldart's group B. To understand turbulent fluidization, knowledge about the bubbling regime is indispensable, because both flow regimes merge into each other gradually and show similarities. For this reason, a detailed insight into the flow structure of bubbling and turbulent fluidized beds is given in this chapter. In the last section existing literature models for turbulent fluidized beds are summarized.

### 2.1 Fundamentals of Gas-Solid Fluidization

Fluidized bed technology is widely applied in industrial processes for chemical conversion and particle formulation. Each process requires certain flow conditions and needs to be designed according to the solid material fluidized. Thereby, a fluidized bed can be operated in different states/flow regimes with particles having different fluidization behavior. Both, the flow regimes and particle classification according to their fluidization behavior are discussed in the following.

#### 2.1.1 Flow Regimes

If gas streams through a packed bed of particles at low velocities, the bed induces a pressure drop. This pressure drop increases if the superficial gas velocity is increased. By reviewing information about the flow of fluids through a packed bed of particles, Ergun [8] found the pressure drop to be caused by kinetic and viscous energy losses, which can be expressed by:

$$\frac{\Delta P}{\Delta h} = 150 \frac{(1 - \epsilon)^2}{\epsilon^3} \frac{\eta_f U_0}{(d_{3,2} \Psi_{Wa})^2} + 1.75 \frac{1 - \epsilon}{\epsilon^3} \frac{\rho_f U_0^2}{d_{3,2} \Psi_{Wa}} \quad (2.1)$$

The pressure drop  $\Delta P$  was found to depend on the height difference  $\Delta h$ , the bed porosity  $\epsilon$ , the gas density  $\rho_f$  and viscosity  $\eta_f$ , the superficial gas velocity  $U_0$ , the Sauter mean diameter of the particles  $d_{3,2}$  (diameter of a particle having

the mean volume to surface area ratio of the particles in a bulk) and the shape factor of the particles  $\Psi_{Wa}$ .

If the superficial gas velocity is increased beyond a certain point, the particle drag force induced by the gas overcomes the gravitational force acting on the particles. Fluidization begins and the flow of gas changes from a stream through the voids of the stationary particle bed into a state of rising gas bubbles leading to gas induced particle movements. The state of minimum fluidization is reached and the superficial gas velocity at this point is called minimum fluidization velocity  $U_{mf}$ . Different approaches for the determination of the minimum fluidization velocity are available in literature [9]. Equation 2.2 gives an approach introduced by Wen and Yu [10]:

$$Re_{mf} = 33.7 \left( \sqrt{1 + 3.6 * 10^{-5} Ar} - 1 \right) \quad (2.2)$$

It sets the Reynolds number at minimum fluidization  $Re_{mf}$  in dependence of the Archimedes number  $Ar$ , which are defined by equations 2.3 and 2.4, respectively.  $\rho_f$  is the gas density,  $\eta_f$  the gas viscosity,  $d_p$  the particle size,  $\rho_s$  the particle density, and  $g$  the gravitational acceleration:

$$Re_{mf} = \frac{\rho_f U_{mf} d_p}{\eta_f}, \quad (2.3)$$

$$Ar = \frac{\rho_f (\rho_s - \rho_f) g d_p^3}{\eta_f^2} \quad (2.4)$$

Gas pockets rise characteristically in the shape of bubbles comparable to large gas bubbles rising in liquids, where effects of surface tension and viscosity are small [11]. For this reason, this state is called bubbling fluidization. It is schematically shown in figure 2.1 (b), where the occurrence of bubbles leads to an expansion of the bed in comparison to the fixed bed flow in (a). Whereas the pressure drop over the bed increases steadily in the fixed bed flow, it is constant in the bubbling regime. The pressure drop  $\Delta P$  of a fluidized bed is induced by the weight of the solid material and can be estimated by [12]:

$$\frac{\Delta P}{\Delta h} = (\rho_s - \rho_f) (1 - \epsilon) g \quad (2.5)$$

Thus, the bed pressure drop depends on the height difference  $\Delta h$ , the solids density  $\rho_s$ , the gas density  $\rho_f$ , the bed voidage  $\epsilon$  and the gravitational acceleration  $g$ .

The bubbles in a bubbling fluidized bed grow in size with increasing superficial gas velocity and distance from the gas distributor due to coalescence. This can

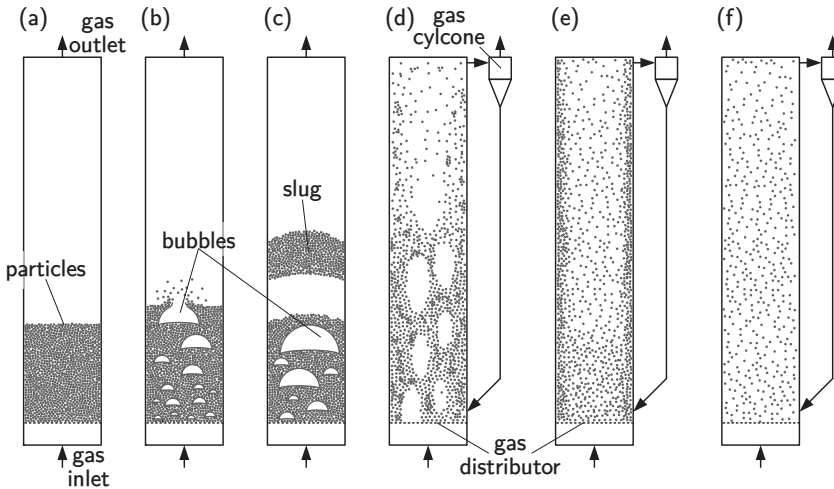


**Fig. 2.1:** Different fluidized bed flow regimes: (a) fixed bed, (b) bubbling, (c) slugging, (d) turbulent, (e) fast and (f) pneumatic conveying.

be seen in measurements and correlations predicting the bubble size [9, 13]. If bubbles reach the size of the diameter of the fluidized bed, slugs of particles rise periodically in the bed until they break and fall down [9]. The slugging fluidization state is reached, shown in figure 2.1 (c). Slugging does not necessarily appear in a fluidized bed because its occurrence strongly depends on the fluidized bed size and bed height [14].

With further increase of the superficial gas velocity the bubbling or slugging regimes merge into the turbulent fluidized bed regime shown in figure 2.1 (d). A change of the clear bubbly flow structure into a more turbulent, diffuse state occurs and pressure fluctuations, which are mainly induced by bubble rise in the bubbling regime, decrease gradually. In this state of fluidization a bed surface is only barely determinable [9]. Particle entrainment plays a role in turbulent fluidized beds and particles should be recirculated into the bed in continuous processes.

Significant particle entrainment with large rates of solid circulation occurs when the turbulent flow changes into a fast fluidization at larger superficial gas velocities (figure 2.1 (e)) [9]. A characteristic core-annulus flow structure with solids rising in a dilute zone in the bed center and descending at larger concentrations at the fluidized bed wall is formed with particles tending to form aggregates and to move as clusters [12].

If the superficial gas velocity is further increased, pneumatic conveying is

reached. In this state particles are transported by the gas in a dilute phase as shown in figure 2.1 (f) [9].

### 2.1.2 Particle Classification according to Geldart

Because particles of different size and density show different fluidization behavior, Geldart [15] introduced a classification of particles into four different groups:

- Particles belonging to **Geldart's group A** usually have a comparably small mean particle diameter and particle densities below  $1400 \text{ kg m}^{-3}$ . If a fixed bed of these particles is streamed through by gas, it expands considerably before bubbling fluidization sets in. Bubbles in these beds rise faster than the interstitial gas velocity and bubbles coalesce and break-up with a maximum bubble size occurring.
- **Geldart's group B** particles are larger than group A particles and have larger densities. The bed does not expand considerably until reaching the minimum fluidization velocity. Bubbles are known to still rise faster than interstitial gas velocity, whereas there is no evidence for a maximum bubble size for this kind of particles.
- Very fine cohesive powders are difficult to fluidize and are classified to **Geldart's group C**. Gas streaming through these powders tends to form channels due to the inter-particle forces being larger than the forces induced by the gas.
- If particles are very large with high particle densities in comparison to the other groups, they are classified to **Geldart's group D**. In beds of these particles bubbles rise slower than the interstitial gas velocity. Thus, they are streamed through by the gas from the bottom to the top.

According to Geldart [15], these four groups can be differentiated in a diagram of particle size  $d_p$  versus particle density  $\rho_s$  minus fluid density  $\rho_f$  as shown in figure 2.2. The borders between the groups A and B and groups B and D are defined as given by:

$$(\rho_s - \rho_f) d_p = 225, \quad (2.6)$$

$$(\rho_s - \rho_f) d_p^2 = 10^6 \quad (2.7)$$

The border between the groups C and A according to Geldart [15] is based on measurement data.

In addition to Geldart, other authors introduced similar definitions for borders between the four groups [9].

Because this work aims on the investigation of fluid dynamics of turbulent

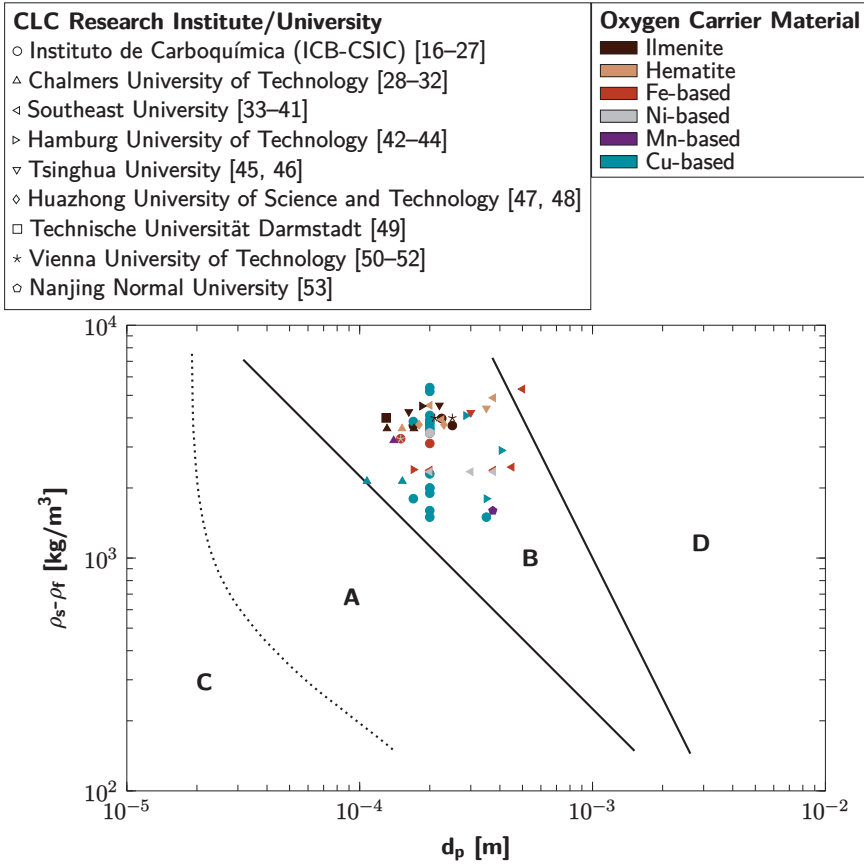


**Fig. 2.2:** Particle classification according to Geldart [15] with its groups C, A, B and D, its group borders according to equations 2.6 (A-B) and 2.7 (B-D) and different oxygen carriers used in literature for chemical looping combustion (CLC).

fluidized beds as fundamental research for chemical looping combustion (CLC), oxygen carriers used for this process are additionally classified in figure 2.2. These oxygen carriers are based on different metals, which usually have high particle densities. A broad range of densities and particle sizes is used in literature with almost all oxygen carriers clearly belonging to group B according to Geldart's classification (in cases where particle density was not available in the study, information from other studies of the same research group was taken). For this reason, bed materials belonging to Geldart's group B are in the center of interest in this work.

## 2.2 Flow Structure of Bubbling Fluidized Beds

The flow structure in turbulent fluidized beds is complex. A dense zone exists in the bottom of the bed. There, gas pockets (which can also be called voids or even bubbles) rise through a suspension phase. With larger distance from the gas distributor the dense zone merges into a dilute zone, which is dominated by a flow of particles entrained from the bed.

The transitions from bubbling to turbulent and from turbulent to fast fluidization do not happen by a sudden change in flow structure. The change in flow structure is smooth and points of the transitions can only be determined by definition of certain criteria, which will be explained in detail later. Thus, to fully understand the development of a turbulent flow in a fluidized bed it is indispensable to understand the flow structure and the behavior of bubbles in bubbling fluidized beds.

### 2.2.1 Generation of Bubbles

Bubbles streaming through the bed are generated at the gas distributor. There are different kinds of gas distributor types commercially available, such as porous plates, perforated plates or bubble cap trays. Depending on the process application, fluidized beds can also be operated with gas injection nozzles. All these different methods of gas distribution/injection into fluidized beds have influence on the generation of bubbles and finally the performance of fluidized bed reactors [11, 54].

A homogeneous gas distribution is preferred for chemical conversion processes to achieve uniform gas-solid contact and also the resulting high heat transfer rates. If gas distribution is inhomogeneous large bubbles can be developed at only one site of the reactor. The main amount of gas inside these bubbles never gets in contact with solid material which decreases conversion rates. To prevent inhomogeneous distribution the pressure drop over the gas distributor should be large compared to bed pressure drop [55].

As described by Karimipour and Pugsley [13], several researchers investigated the initial sizes of bubbles formed at the distributor. Werther and Molerus [56] observed formation of bubbles in small distance above the gas distributor (in this case porous plate) with an initial size of 3-5 mm depending on superficial gas velocity. In a further study, these authors found non-uniform bubble development at the gas distributor [55]. A region of pronounced bubble development close to the wall was observed independent of the gas distributor to bed pressure drop ratio and the size of the fluidized bed. Werther and Molerus [55] explain this behavior with altered packing geometry of particles and different conditions